Bare Demo of IEEEtran.cls for IEEE Computer Society Conferences

Isaac Sacramento
and Mauro Roisenberg
and Rodrigo Exterkoetter
Departament of Computer Science
Federal University of Santa Catarina
Florianopolis, Santa Catarina
Email: isaac.sacramento@posgrad.ufsc.br

Leando P. de Figueiredo
Departament of Physics
Federal University of Santa Catarina
Florianopolis, Santa Catarina
Email: homer@thesimpsons.com

***Abstract*—In this paper we will present a new convolution neural network model to deblurr post-insversion acoustic impedance images.**

1. Introduction

Deblurring is an important problem in image processing. It seeks to remove distortions from a blurry image in order to recover the original image. Recovering the original image is possible if the details of the blurring method are known. In most cases, blurred images lack of enough information to uniquely recover a plausible image, this feature sets deblurring as an ill-posed problem and characterizes as an inversion problem. It is not observed in the literature a general object deblurring algorithm. Thus, as mentioned by [6] exploiting domain-specific knowledge can result in superior deblurring. The focus of this work is post-inversion acoustic impedance deblurring. Specifically, acoustic impedance deblurring must take into account the fact that the resulting image still must to reflect the synthetic seismic data characteristics.

Reservoir characterization consists in determining the multidimensional and quantitative structure and properties of an oil field. To achieve this goal, it is essential to combine in a single model all the information, knowledge and data about the field, in such a way that is possible to make the quantitative predictions about the reservoir behavior [8]. These data are usually geological models, data logs, testimonial data, production summary and 3D seismic data. The seismic amplitude is used in model generation and reservoir characterization, however, the deeper the investigated horizon is, the bigger the limit in using the seismic amplitude data [9]. The seismic data inversion has proved to be an efficient tool to accurately integrate the seismic information in order to generate models that contribute to an effective reservoir characterization [10]. Besides integrating data, seismic inversion is widely used because of its facility and precision in interpreting the acoustic impedance. According to [7], a good acoustic impedance model contains more information then the seismic data because this model keeps all the seismic data information and additional information originated in the well-logs. Depending on the applied method, the acoustic impedance volume is the result of the integration of data from different sources, such as, the seismic data, well logs and velocity models. Thus, building an acoustic impedance model is the natural process to integrate the available informations to obtain a model accessible to geophysicists, geologists and engineers. The acoustic impedance models allow fast interpretations and an efficient identification of exploratory targets in seismic scale. However, the seismic data are band-limited, in other words, the seismic data are short of high and low frequencies. This is a consequence of seismic acquisition, earth attenuation, high-frequency noise, etc [2]. This phenomenon leads to a misinterpretation of seismic data and, by consequence, the same to the resulting acoustic impedance models, that lacks of high-frequency details, additionally, inversion methods such as MAP (Maximum a posteriori), lead to blurry images [16]. In this sense, we believe that increasing the resolution of the acoustic impedance models through deblurring the model sections, as a post-inversion refining process, can lead to a more accurate interpretation of the impedance models.

We approach the problem of deblurring post-inversion acoustic impedance images through the Convolution Neural Networks (CNN). CNN is a framework of deep learning which has been used in a wide sort of machine learning tasks. The availability of benchmarks [11] and the advances in Graphical Processing Unit (GPU) [3] allowed CNN to outperform techniques in detection [12], [13], model-free tracking [14], classification [15]. With excellence in feature learning, CNN achieved notorious success in image classification [17], action recognition [18], video classification [19] and speech recognition [20]. Under the post-inversion perspective, we consider acoustic impedance as image and work on it with image processing algorithms.

In this paper we propose a new multilayer convolution network model to perform deblurring in post-inversion

acoustic impedance. Each network layer maps higher level features originated in the previews layers through convolutional filters. To perform this mapping, the filters, also named weights, are adjusted by minimizing a loss function. The trained model enhances the resolution of the impedance image, resulting in an equivalent image with increased high-frequency band and lower noise. First, we blurr the synthetic acoustic impedance to form the pairs of images of high and low resolution. Then, the dictionary of images is normalized to the real interval $[0, 1]$ and used to train the convolutional model. We compare the deblurred images depicted by our model and by two other deblurring methods (). The core concept of our architecture is the combination of the convolution layers with regression layers, thus proceeding a regression solution, instead of classification.

2. Related Work

Deblurring plays an important role in computer vision. Methods based on...However these methods lack of ...

Recent researches in geophysics have applied deep learning solutions, such as convolution networks, to solve a wide sort of problems such as lithofacies recognition [4] and calculation [5].

However, there is a lack of researches to investigate methods for improving the resolution of images resulting from inversion processes. According to [2], improving the resolution of seismic inversion is possible by adding high frequency in acquisition and processing seismic data. The seismic data is generally short of high and low frequencies and this phenomenon is caused by seismic acquisition, earth attenuation, high-frequency noise, etc., what negatively influence on geologic interpretations of seismic data. Thus, we propose enhancing seismic impedance resolution through adding high-frequency as a post-inversion.

3. Data and Method

3.1. Acoustic Impedance Inversion

The experiments described in this paper were performed on a set of synthetic acoustic impedance images. Using synthetic models to test and parametrize algorithms is a common practice in reservoir characterization [10]. It allows to study the results of the algorithms without external interferences and to obtain efficient interpretations and assessments. According to [21], wedge shaped models is a straight way to analysis the seismic model modeling and inversion processes. It realistically reproduces reservoir contexts such as stratigraphic refinements, *pich-outs* in sand layers, edges and channel structures.

In order to generate a set of training image pairs, we proceed two steps to obtain the wedge images. In the fist step we create a set of random wedges forms, containing two horizontal dimensions represented in images 32 x 32. The wedges representing the reservoir varied randomly in width and length. The second step filled the lithology with

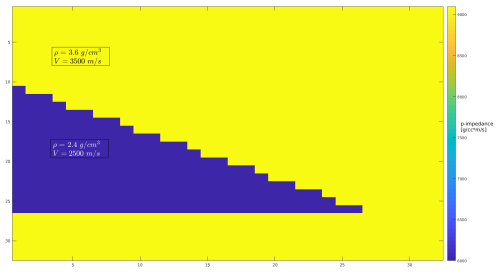

Figure 1. Acoustic impedance blurred model.

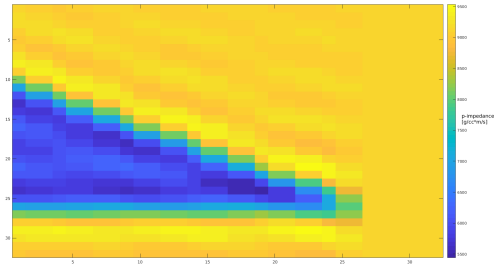

Figure 2. Acoustic impedance blurred model.

values of petrophysical properties. In order to simplify the assessments and conclusions, the lithology structures are filled with constant reference values of rock densities and compressional velocity observed in the literature. With the density and velocity models the acoustic impedance is calculated and a high resolution model is obtained. Fig. 1 illustrate the lithology model with the corresponding values for density and velocity.

In a real scenario, the blurred acoustic impedance is the result of an inversion method, that might be Maximum a Posteriori [], Sparse Spike [] and Recursive Inversion []. However, for experimental purpose, the acoustic impedance models were low-passed filtered and the high frequencies were removed, this way we proceed the supervised training with high resolution and blurred images. The blurred image is illustrated in Fig. 2. To increase the number of examples in the training dataset we rotate the impedance models in integer multiples of right angle. This approach allows the model learning the maximum edge variabilities in wedges images.

3.2. Convolutional Neural Network

The work-flow of the proposed method consists of the following steps:

- Generate the synthetic impedance images;
- Blurr the images through a low-pass filter;
- Train the convolutional model with the pair of high and low resolution images;
- Test the model with different blurry images;

- Assess the result for the testing output.

The CNN is a well established method for patter recognition and image classification. Thus, an important breakthrough when applying CNN to deal with physical property images is developing a model capable to solve regression tasks. The model presented in this paper is able to solve two important problems related to deblurring physical properties images: (1) learning the spacial patterns in the low resolution training images and (2) predicting each pixel intensity value in the new higher resolution image. To reach these two goals, the architecture of the CNN contains convolutional layers combined with a regression output layer.

The model proceeds a supervised learning through a dictionary containing pairs of low and high resolution images. The optimization algorithm adjusts the network weights in every layer by minimizing the Mean Squared Error (MSE) in each batch of images. Thus, after the training phase, the model is capable to deblurr any other image not presented in training dataset. The output image recovers the high frequencies and presents higher similarity to the high resolution image than to the blurred image, according to stablished metric. The model was adjusted to deblurr a wide variety of wedges shapes and impedance values. Those wedges which the model was unable to predict were added in the training set.

Three metrics assess the performance of the convolution networks: Fast Fourier Transform Index (FFTI), the Rooted Mean Square Error (RMSE) and the frequencies magnitudes. The FFTI is a similarity metric calculated based on the Fast Fourier Transform (FFT) of each image. It is introduced by [22] and calculates as in Eq. 1

$$C = \frac{(\sum_{i=1}^{N} F_{1i}F_{2i} - N\bar{F}_1\bar{F}_2)^2}{(\sum_{i=1}^{N} |F_{1i}|^2 - N\bar{F}_1^2)(\sum_{i=1}^{N} |F_{2i}|^2 - N\bar{F}_2^2)}, \quad (1)$$

where, for each frequency, an intensity value is calculated from the real and complex parts of fourier transform. F_{1i} represents the intensity value of i-th *pixel* in the first image and F_{2i} is the intensity value of i-th *pixel* in the second image. $\bar{F}_1$ e $\bar{F}_2$ are the mean frequencies in each image. The closer FFTI is to 1, the higher the similarity between the images. The frequencies spectrum is additionally useful to present the graphic of frequency magnitudes in the images. The frequency magnitude graphic allows distinguishing what high frequencies were added to the acoustic impedance after the low resolution image is passed through the trained CNN. Additionally, the Root Mean Squared Error (RMSE) in Eq. 2 is calculated in order to measure the global error in each pair of deblurred and high resolution images.

$$RMSE = \sqrt{\frac{(\sum_{i=1}^{N} (x_i - y_i)^2}{N}}, \quad (2)$$

The model architecture consists in two convolution layers, each one followed by one pooling layer and a regularization layer. The second regularization layer is followed by a fully connected layer, which maps the convolution layer's output to 1024 neurons. The output model comprises a regression layer to predict the intensity value of each pixel.

4. Experiments

This section describes the experiments and results obtained with the proposed method. We compare the results with the state-of-the-art deblurring algorithms in four different scenarios.

In the first scenario we trained and tested the network with images of acoustic impedance normalized to 0 and 1. This scenario evaluated the model capability to deblurr lithology with similar acoustic impedance values as in the training dataset, but with different shapes. In the second scenario, we inverted the lithology impedance values in the test images to evaluate the ability of the network to predict the correct impedance value, despite the position of the a pixel on the image.

In the third scenario, we kept the training dataset, but tested with images impedance values normalized to 0.3 and 0.7. In this scenario assess the ability of the network in extrapolating the prediction of impedance values to a range not presented in the training dataset.

The fourth scenario tested images with different acoustic impedance values and different wedge shapes and rotations, in comparison to the images used in the training phase. In this case we tested the model capability to deblurr different wedge shapes, located in different positions, and to extrapolate the acoustic impedance values.

4.1. Implementation Details

The model was implemented using the Deep Learning toolbox delivered in MATLAB R2017A. For training the network, we used a mini-batch with size of 32 training examples; the network weights are randomly initialized and the Stochastic Gradient Descendant with Momentum (SGDM) [23]. We adopted an exponentially decreasing learning rate (initially set to 0.005), and decreasing every iteration in a total of 100 iterations. It should be noted that, once the wedge shapes are generated randomly, every image is different and was introduced only once to the network, this way avoiding over-fitting.

4.2. Integer Angles Rotated Wedges

We adopted an incremental approach for building a consistent convolutional model. The initial model was composed by the input layer, one convolutional layer, one max-pooling layer, a fully connected layer and the output layer mapped to 1024 output neurons. To build the training dataset, we generated 500 random wedge images, these were rotated in integer multiple of 90 degrees, making a total of 2000 images. The rotated images were blurred by applying a low-pass filter with cut frequency $4Hz$ and the pairs of blurred and not-blurred images were used to adjust the model weights. The same process was applied to generate 4 testing images.

The first scenario we tested the model with acoustic impedance images with the same features of the images in the training dataset, that means, the same rotation and the

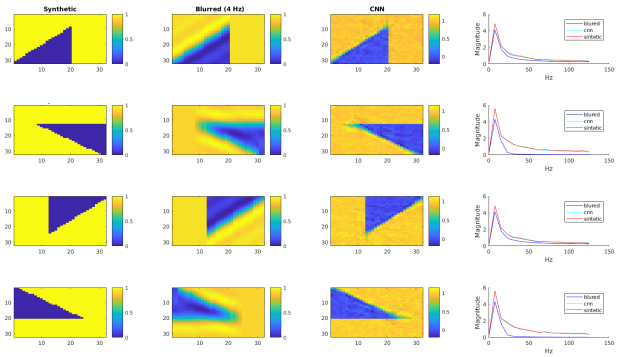

Figure 3. Acoustic impedance blurred model.

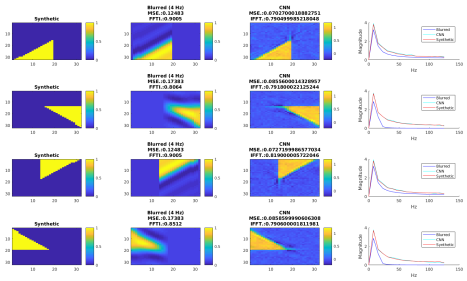

Figure 4. Inverted acoustic impedance values blurred model.

same impedance values. The wedges in the testing set differ from the the ones in the training set only by their shapes. Fig. 3 presents the result obtained with the initial model applied to the test images. The first column shows the high resolution images followed by the blurred images, the third column shows the result of the convolutional deblurring network and the fourth column shows the graph of frequency magnitudes. The global error for each image in comparison to the high resolution image is presented on top of it, as well as, the fourier metric FFTI.

In the second scenario, we inverted the impedance values of the lithology structures. This experiment showed the network capacity to predict the correct value of a pixel based only on the value of the input pixel. This way we verified that the pixel value is disconnected to the lithology shape. Fig. 4 shows the results obtained in this scenario.

In the third scenario, we arbitrarily changed the normalized impedance to values of higher impedance out of the wedge (with value of 0.3) and lower impedance (with value of 0.7) into the lithology structure. These values are out the range learned by the model during the training phase. Doing this, we tested the model generalization capacity to reach the learned pixel intensity values. We observed that, once the model is trained with pixel valued to 0 and 1, the network poorly extrapolated and a new training dataset was generated containing wedges with the new pixel values.

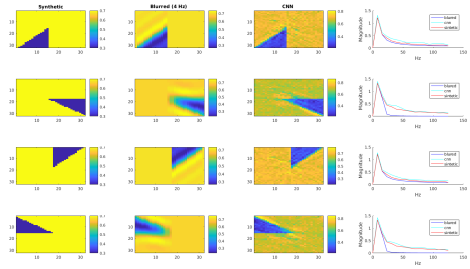

Figure 5. Acoustic impedance blurred model.

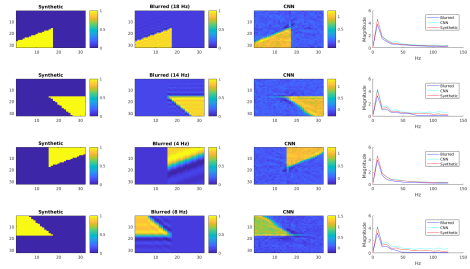

Figure 6. Acoustic impedance blurred model.

The Fig. 5 shows the result for the network trained with the extended dataset.

We also simulated the scenario in which the synthetic images were blurred with different cut frequencies. This is of particular interest, once the different blurring aspects may occur in post-inversion images, as the result of attenuation and reflectivity in deeper subsurface layers. Fig. 6 shows the results for this scenarios.

4.3. Randomly Rotated Wedges

Randomly rotated wedge is related to a lithology positioned in a random angle. In this case, we evaluated the CNN capability to deblurr the lithology with unknown shape and position. Unknown, means that test cases presented in this section did not integrate the training dataset. Thus, we simulated a wedge completely immersed in a second lithology. The model was trained with lithologies rotated in integer multiple of the right angle. and with both range of normalized impedance $[0, 1]$ and $[0.3, 0.7]$. Thus, we expected that the model recover the correct values for both lithologies, and extrapolate the identification of edges and contours of the wedges.

Fig. 7 shows the test case in which the acoustic impedance was generated with values 0 and 1. As the network was trained with wedges with the same value, the network was able to predict the pixel intensity value.

Fig. 8 shows the test case in which the wedges were positioned in random angles and the acoustic impedance was normalized to values equal to 0.3 and 0.7. These values were not present in the training dataset and it notable a wider

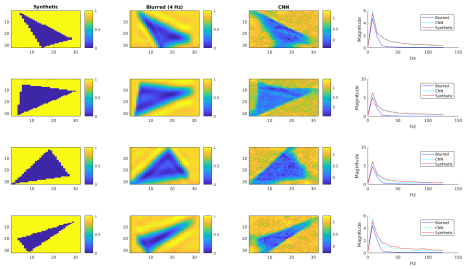

Figure 7. Acoustic impedance blurred model.

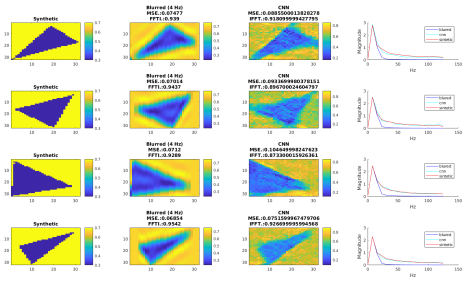

Figure 8. Acoustic impedance blurred model.

spread of values in both lithologies outputed by the network.

5. Conclusion

The conclusion goes here.

Acknowledgments

The authors would like to thank...

References

[1] H. Kopka and P. W. Daly, *A Guide to LaTeX*, 3rd ed. Harlow, England: Addison-Wesley, 1999.

[2] Xi Xiaoyu, Ling Yun, Sun Desheng, Guo Xiangyu, and Wang Huifeng, "Studying the effect of expanding low or high frequency on post-stack seismic inversion," in SEG Technical Program Expanded Abstracts 2012. September 2012, 1-5.

[3] Buduma, N., " Fundamentals of Deep Learning," Academic Press, 2015, in O'Reilly Media.

[4] Qian Feng, Yin Miao, Su Ming-Jun, Wang Yaojun, Hu Guangmin, "Seismic facies recognition based on prestack data using deep convolutional autoencoder,".

[5] Liu Lihui, Lu Rong, Li Jianhai, Yang Wenkui, "Seismic Lithofacies Computation Method Based on Deep Learning," p. 649-652.

[6] G. G. Chrysos, S. Zafeiriou, "Deep Face Deblurring," 2017 IEEE Conference on Computer Vision and Pattern Recognition Workshops (CVPRW), Honolulu, HI, 2017, pp. 2015-2024.

[7] Rebecca Buxton Latimer, Rick Davidson, Paul van Riel, "An interpreter's guide to understanding and working with seismic-derived acoustic impedance data,",2017, pp. 242-256, v. 19, num. 3, in The Leading Edge.

[8] JJM. Buiting, M. Bacon,"Using geophysical, geological, and petrophysical data to characterize reservoirs in the North Sea.", in 5th Conference on Petroleum Geology of NW Europe, London. CD-ROM.

[9] Paul van Riel, "The past, present and future of quantitative reservoir characterization.", in The Leading Edge, 19, p. 878881.

[10] Sergio Sacani Sancevero, Armando Zaupa Remacre, Rodrigo de Souza Portugal, "O papel da inverso para a impedncia no processo de caracterizao ssmica de reservatrios",in Revista Brasileira de Geofsica, 2006, p. 495-512, v. 24.

[11] O. Russakovsky, J. Deng, H. Su, J. Krause, S. Satheesh, S. Ma, Z. Huang, A. Karpathy, A. Khosla, M. Bernstein, "Imagenet large scale visual recognition challenge," in ternational Journal of Computer Vision (IJCV), p. 211252, 2015.

[12] R. Girshick, "Fast r-cnn," In IEEE Proceedings of International Conference on Computer Vision (ICCV), pages 14401448, 2015.

[13] S. Bell, C. L. Zitnick, K. Bala, and R. Girshick, "Inside-outside net: Detecting objects in context with skip pooling and recurrent neural networks," in arXiv preprint arXiv:1512.04143, 2015.s

[14] H. Nam and B. Han, "Learning multi-domain convolutional neural networks for visual tracking," In IEEE Proceedings of International Conference on Computer Vision and Pattern Recognition (CVPR). IEEE, 2016.

[15] K. He, X. Zhang, S. Ren, and J. Sun, "Deep residual learning for image recognition," In IEEE Proceedings of International Conference on Computer Vision and Pattern Recognition (CVPR). IEEE, 2016.

[16] A. Levin, Y. Weiss, F. Durand, and W. T. Freeman. Understanding and evaluating blind deconvolution algorithms. In IEEE Proceedings of International Conference on Computer Vision and Pattern Recognition (CVPR), p. 19641971.

[17] A. Krizhevsky, I. Sutskever, G. E. Hinton, "Imagenet classification with deep convolutional neural networks: Advances in neural information processing systems," 2012, p. 10971105.

[18] S. Ji,W. Xu, M. Yang, K. Yu, 2013, "3d convolutional neural networks for human action recognition," in IEEE transactions on pattern analysis and machine intelligence, n. 35, p. 221231.

[19] O. Abdel-Hamid, A.-r. Mohamed, H. Jiang, L. Deng, G. Penn, D. Yu, 2014, "Convolutional neural networks for speech recognition," in IEEE/ACM Transactions on audio, speech, and language processing, n. 22, p. 15331545.

[20] S. S. Farfade, M. J. Saberian, L.-J. Li, 2015, "Multi-view face detection using deep convolutional neural networks," in Proceedings of the 5th ACM on International Conference on Multimedia Retrieval, ACM, p. 643650.

[21] P. J. Harvey, D. J. MacDONALD, "Seismic modelling of porosity within the jurassic aged carbonate bank, offshore Nova Scotia," in Canadian Journal of Exploration Geophysics, n. 26, p. 5471.

[22] S. Narayana, P. K. Thirivikraman, "Image similarity using fourier transform," in International Journal of Computer Engeneering and Technology, 2015, n. 6, p. 2937.

[23] N. Qian, "On the momentum term in gradient descent learning algorithms," in Neural Networks, v. 12, i. 1, 1999, p. 145-151.